Joint horizontal-vertical anisotropic scaling, isobaric and isoheight wind statistics from aircraft data

J. Pinel,[1] S. Lovejoy,[1] D. Schertzer,[2] and A. F. Tuck[3]

Received 23 March 2012; revised 1 May 2012; accepted 15 May 2012; published 8 June 2012.

[1] Aircraft measurements of the horizontal wind have consistently found transitions from roughly $k^{-5/3}$ to $k^{-2.4}$ spectra at scales Δx_c ranging from about 100–500 km. Since drop sondes find $k^{-2.4}$ spectra in the vertical, the simplest explanation is that the aircraft follow gently sloping trajectories (such as isobars) so that at large scales, they estimate vertical rather than horizontal spectra. In order to directly test this hypothesis, we used over 14500 flight segments from GPS and TAMDAR sensor equipped commercial aircraft. We directly estimate the joint horizontal-vertical (Δx, Δz) wind structure function finding - for both longitudinal and transverse components - that the ratio of horizontal to vertical scaling exponents is $H_z \approx 0.57 \pm 0.02$, close to the theoretical prediction of the 23/9D turbulence model which predicts $H_z = 5/9 = 0.555\ldots$. This model also predicts that isobars and isoheight statistics will diverge after Δx_c; using the observed fractal dimension of the isobars ($\approx 1.79 \pm 0.02$), we find that the isobaric scaling exponents are almost exactly as predicted theoretically and $\Delta x_c \approx 160$, 125 km, (transverse, longitudinal). These results thus give strong direct support to the 23/9D scaling stratification model.
Citation: Pinel, J., S. Lovejoy, D. Schertzer, and A. F. Tuck (2012), Joint horizontal-vertical anisotropic scaling, isobaric and isoheight wind statistics from aircraft data, *Geophys. Res. Lett.*, *39*, L11803, doi:10.1029/2012GL051689.

1. Introduction

[2] The classical laws of turbulence exploit the scale invariance of the dynamical equations to predict the scaling behaviour of the wind and other turbulent fields. For simplicity, they also assume statistical rotational invariance: isotropy. When applying these laws to the strongly stratified atmosphere, one faces a choice: to drop either the scaling or the isotropy symmetry. Starting with the claimed discovery of the meso-scale gap [*Van der Hoven*, 1957], and the subsequent development of theories of 2D (isotropic) turbulence [*Kraichnan*, 1967] - and especially Charney's geostrophic variant [*Charney*, 1971] - the dominant choice was to drop the scaling symmetry, to assume that the small scale dynamics were 3D isotropic and the large scale 2D isotropic with a scale break somewhere near the atmospheric scale height (≈10 km).

[3] Starting in the early 1980's the opposite proposal was made [*Schertzer and Lovejoy*, 1985b, 1987]: to drop isotropy but to maintain wide range horizontal scaling. In this framework, the vertical structure was also expected to be scaling but with different exponents than the horizontal. Since then, evidence in the horizontal and vertical from satellites, lidar, aircraft, radiosondes, drop sondes and reanalyses has accumulated, supporting the anisotropic scaling model (see the review by *Lovejoy and Schertzer* [2010] and also by *Tuck* [2008]). More recently, an (anisotropic) *scaling* (rather than a traditional *scale*) analysis of the governing equations [*Schertzer et al.*, 2012] has allowed the derivation of new fractional vorticity equations with anisotropic scaling solutions.

[4] Until recently, the outstanding piece of evidence supporting the isotropic 2D/3D model and potentially falsifying the anisotropic scaling hypothesis was the observed break in aircraft spectra of the horizontal wind at scales of several hundred kilometers. However, using high quality scientific aircraft data, *Lovejoy et al.* [2004, 2009a] argued that the aircraft trajectories - and hence the wind measurements - would be affected by the turbulence and they predicted a transition from $k^{-\beta_{\text{small}}}$ spectra with $\beta_{\text{h}} \sim 5/3$ and $\beta_{\text{small}} \sim \beta_{\text{h}}$ at small horizontal scales to $k^{-\beta_{\text{large}}}$ spectra at large scales where the aircraft essentially sensed the vertical rather than horizontal fluctuations; with vertical exponent $\beta_v \sim 2.4$ and $\beta_{large} \sim \beta_v$. They also showed that essentially all the horizontal wind spectra and structure functions published to date were compatible with this transition – but not with the more drastic transition from $\beta_{small} = 5/3$ to $\beta_{large} = 3$ near 10 km predicted by the competing 2D/3D model.

[5] The paper by *Lovejoy et al.* [2009a] sparked a debate [*Lindborg et al.*, 2009, 2010; *Lovejoy et al.*, 2009b, 2009c, 2010; *Schertzer et al.*, 2011, 2012; *Yano*, 2009] and provoked *Frehlich and Sharman* [2010, hereinafter FS] to perform a new analysis using Tropospheric Airborne Meteorological Data Reporting (TAMDAR) commercial aircraft data. The key new element was that the TAMDAR data had GPS altimetry and were thus – for the first time for commercial aircraft – able to adequately distinguish isobaric and isoheight statistics. This is important because most aircraft follow isobars and these are gently sloping. If these slopes are large enough, then the aircraft spectra will show a spurious transition from β_h to β_v at a scale which depends on the slope and the turbulent fluxes, thus explaining the observations. FS found neither a scale break near 10 km nor a structure function with exponent anywhere near 2 (corresponding to $\beta_{large} = 3$) – so that presumably

[1]Physics Department, McGill University, Montreal, Quebec, Canada.
[2]LEESU, Ecole des Ponts ParisTech, Université Paris-Est, Marne-la-Vallée, France.
[3]Physics Department, Imperial College London, London, UK.

Corresponding author: J. Pinel, Physics Department, McGill University, 3600 University St., Montreal, QC H3A 2T8, Canada. (ze.pinel@gmail.com)

there was not a 2D/3D transition. However, they did make the strong claim that the statistics on isobars and isoheights were identical. If their claim was true, then another mechanism to account for the $k^{-5/3}$ to $k^{-2.4}$ transition would be required.

[6] However, distinguishing the statistics on isoheights and isobars requires very high accuracy – both of wind but especially altitude – measurements. These accuracy requirements are too demanding for the older Aircraft Meteorological Data Relay (AMDAR) equipment (also discussed by FS). With the newer GPS equipped TAMDAR data, the requisite accuracy is possible to achieve if two conditions are met. First, we do not use wind differences from two *different* aircraft since this involves both larger (absolute) errors as well as nontrivial complications due to the very inhomogeneous distribution of TAMDAR flights paths over the US: the errors are unacceptably large. Second, the TAMDAR sampling protocol was ill adapted for our purpose, it was essential to use only the high quality "cruise" flight segments. Unfortunately, the copiously sampled ascent and descent segments had to be discarded because of their unacceptably low vertical resolutions (see Figure S3 in the auxiliary material).[1] Using two aircraft differences and these low resolution segments, we could accurately reproduce the FS TAMDAR results (see Figures S1 and S2 in the auxiliary material).

[7] Finally, we could mention that *Lovejoy and Schertzer* [2010] examined hydrostatic models and found that they also gave isobaric exponent $\beta \sim 2.4$ and *Lovejoy and Schertzer* [2011] confirmed this in reanalyses, although with an extra complication due to a strong *horizontal* (zonal/meridional) scaling anisotropy (i.e., different exponents in orthogonal *horizontal* directions); so that these data are not appropriate for distinguishing isoheight and isobaric statistics. With these differences, we therefore redid the FS TAMDAR analyses.

2. Generalized Scale Invariance

[8] Isotropic turbulent laws are of the general type: $\Delta v = f|\Delta \boldsymbol{r}|^{\mathrm{H}}$, where Δv is a fluctuation in a turbulent field v, f is a scale by scale conserved turbulent flux, $|\Delta \boldsymbol{r}| = |(\Delta x, \Delta z)|$ is the length of the horizontal, vertical lag vector over which Δv is calculated (for simplicity, we consider only a single horizontal component) and H is the scaling (non conservation, mean fluctuation) exponent. Anisotropic scaling turbulence has different vertical ($\mathrm{H_v}$) and horizontal ($\mathrm{H_h}$) exponents which result when different conserved turbulent fluxes dominate the corresponding dynamics, for example:

$$\Delta v(\Delta x) = \varepsilon^{1/3}\Delta x^{\mathrm{H_h}}$$
$$\Delta v(\Delta z) = \phi^{1/5}\Delta z^{\mathrm{H_v}} \quad (1)$$

where ε and ϕ are the energy and buoyancy variance fluxes (i.e., $f = \varepsilon^{1/3}$, $\phi^{1/5}$ respectively and $\mathrm{H_h} = 1/3$, $\mathrm{H_v} = 3/5$). The horizontal law is the Kolmogorov, 1941 scaling and the vertical is the Bolgiano-Obukhov, 1959 scaling. The way to deal with this anisotropy while keeping an overall scaling symmetry is to replace the usual vector norm for the spatial separation by a different measure of scale – the (anisotropic) scale function – a simple example for verticals section is:

$$[[\Delta \boldsymbol{r}]] = l_s\left\{|\Delta x/l_s| + |\Delta z/l_s|^{1/H_z}\right\} \quad (2)$$

where $\mathrm{H_z} = \mathrm{H_h}/\mathrm{H_v} = 5/9$ and l_s is the "sphero-scale": the scale at which structures are "roundish". (If needed, the scale function can be generalized for full space-time vector displacements). The anisotropy is reflected by the exponent $\mathrm{H_z} \neq 1$ that describes the stratification of structures. Since $\mathrm{H_z} < 1$, at scales much smaller than l_s, structures tend to be vertically aligned whereas at scales much larger than l_s, they become horizontally flatter. With this scale function, we can write:

$$\Delta v(\Delta \boldsymbol{r}) = \varepsilon^{1/3}[[\Delta \boldsymbol{r}]]^{1/3} \quad (3)$$

which, for $\Delta \boldsymbol{r} = (\Delta x, 0)$, $\Delta \boldsymbol{r} = (0, \Delta z)$ reduces to equation (1). The vertical extent of structures of horizontal size L is L^{H_z}; their volumes are $L^{D_{el}}$ with $\mathrm{D_{el}} = 2 + \mathrm{H_z} = 23/9$; this is the 23/9D model [*Schertzer and Lovejoy*, 1985a, 1985b]).

3. Data Analysis

[9] TAMDAR equipped aircraft make short range flights at low altitudes mostly below 7 km; their sensors are the most modern in the AMDAR programme [*Moninger et al.*, 2008; *Daniels et al.*, 2004] and were designed to measure atmospheric fields including wind, humidity, pressure and temperature, as well as location, time and altitude from a built-in GPS. The sampling protocol is important to understand: the system either makes measurements due to significant changes in pressure (changes of 10 hPa or 50 hPa, depending on the altitude) or – if cruising at nearly constant pressure – it switches to a time-based protocol, making measurements every 3 or 7 minutes (again, depending on the level). For an aircraft flying at 500 km/h at an altitude of 5.5 km, the former corresponds to ~25 km. We analysed data for the year 2009 over roughly the continental US (20°N to 50°N latitude). In order to have good statistics and to minimize the strong altitude dependence, we confined our analysis to the layer between 5 and 5.5 km altitude using over 14500 aircraft legs. Only the highest quality data (according to automated quality control checks) were kept.

[10] A nonobvious problem arises since the data were passed through a 10 second smoother, so that measurements at 250 km/h and angle of 15° correspond to a section 180 m thick. Including these low resolution segments led to biases of 7% at 200 km, but this rapidly increased to 67% at 400 km, hence we discarded them (Figure S3 in the auxiliary material). This bias, their use of multi-aircraft data pairs and the fact that FS took much thicker layers for isobars and isoheights (4 hPa, 200 m) compared to those used here (1.26 hPa, 20 m) led to our qualitatively different conclusions (Figures S1 and S2 in the auxiliary material). Similarly to FS, we took only time intervals less than 1 hour to limit the effects of noninstantaneous measurements.

[11] From the near-constant altitude and near-constant pressure levels, we estimated second order structure functions $\mathrm{D_{ii}} = \langle|\Delta v_i(\Delta \boldsymbol{r})|^2\rangle = \langle|v_i(\boldsymbol{r} + \Delta \boldsymbol{r}) - v_i(\boldsymbol{r})|^2\rangle$ where $\langle\cdot\rangle$ means ensemble average, i = N,L for transverse,

[1] Auxiliary materials are available in the HTML. doi:10.1029/2012GL051689.

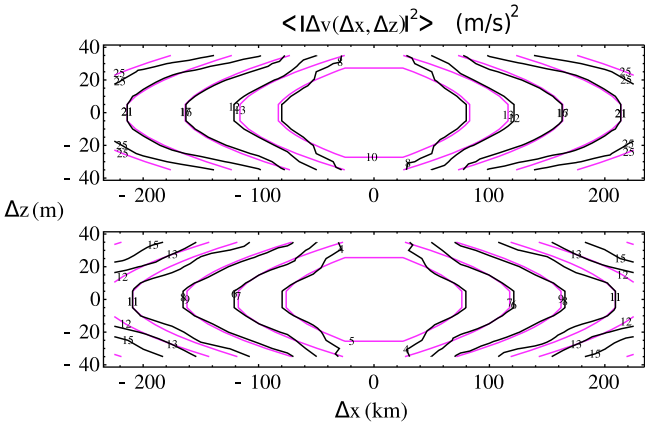

Figure 1. Contour plot of $\langle|\Delta v(\Delta x, \Delta z)|^2\rangle$, in black: horizontal wind measured by TAMDAR. In purple, a fit with the help of the scale function (equations (2) and (3)). (top) Transverse component. (bottom) Longitudinal component. Parameters are: $l_{s,N} \sim l_{s,L} \sim 1.0 \pm 0.1$ mm, $\zeta_h(2) = 0.8$ (from 1D structure functions fits) and $H_{z,N} \sim H_{z,L} \sim 0.57 \pm 0.02$ and $\langle \varepsilon_N^{2/3}\rangle^{3/2} \sim (10 \pm 1) \times 10^{-6}$ m^2/s^3, $\langle \varepsilon_L^{2/3}\rangle^{3/2} \sim (4.0 \pm 0.8) \times 10^{-6}$ m^2/s^3. The average relative error between fitted and empirical curves, the mean of $\frac{\left|\langle|\Delta v|^2_{fit}\rangle - \langle|\Delta v|^2_{emp}\rangle\right|}{|\Delta v|^2_{fit}}$ is ~6% (4%) for transverse (longitudinal) component. The numbers are the values of the contours.

longitudinal components respectively. The accuracies were estimated from the structure function at small enough lags; per component, the absolute calibration error is ≈±1.8 m/s, the relative calibration error is <±1.8 m/s and the altitude error is ≈±3 m (close to the manufacturer's values ±2–3 m/s on wind speed and ±3 m on altitude [*Daniels et al.*, 2004]). To eliminate the absolute calibration errors and numerous other problems introduced by the highly nonuniform distribution of TAMDAR trajectories, we always computed velocity increments with data coming from the same aircraft.

4. Results

[12] Taking ensemble averages of the square of equation (3), we obtain:

$$\left\langle |\Delta v(\Delta \boldsymbol{r})|^2 \right\rangle = \left\langle \varepsilon^{2/3} \right\rangle [[\Delta \boldsymbol{r}]]^{2H_h} = \left\langle |\Delta v(l_s)|^2 \right\rangle \left\{ |\Delta x/l_s| + |\Delta z/l_s|^{1/H_z} \right\}^{\zeta_h(2)} \quad (4)$$

where $\zeta_h(2)$ is the second order structure function exponent which takes into account the intermittency of ε. Since $\langle \varepsilon^{2/3}\rangle \sim [[\Delta \boldsymbol{r}]]^{-K_\varepsilon(2/3)}$, we have $\zeta_h(2) = 2H_h - K_\varepsilon(2/3)$ where $K_\varepsilon(2/3)$ is a small intermittency exponent (~−0.07 [see *Lovejoy et al.*, 2010]). From its definition and the assumption of statistical translational invariance, $\langle|\Delta v(\Delta \boldsymbol{r})|^2\rangle = \langle|\Delta v(-\Delta \boldsymbol{r})|^2\rangle$; we also assumed left-right symmetry so that the four quadrants of $\langle|\Delta v(\Delta x, \Delta z)|^2\rangle$ are symmetric. In order to test the theory, we estimated the parameters in equation (4) by regression. First, $\zeta_h(2)$ was estimated from linear regression using 1D structure functions (Figure 3a), yielding $\zeta_{h,N}(2) = 0.81 \pm 0.02$ and $\zeta_{h,L}(2) = 0.76 \pm 0.03$ which are close to the Kolmogorov value corrected for intermittency $2H_h + 0.07 \approx 0.74$. Only vector lags with at least 500 independent aircraft Δv^2 estimates were used, the average number over the regression range 16 km < Δx < 400 km – see Figure 3 – was 24800. Since presumably $\zeta_{h,N}(2) = \zeta_{h,L}(2)$, we took the value $\zeta_h(2) = 0.8$. Then, from multivariate regression on the joint lags (cross-section, Figure 1), we obtained $H_{z,N} \sim H_{z,L} \sim 0.57 \pm 0.02$, $l_{s,N} \sim l_{s,L} \sim 1.0 \pm 0.1$ mm and $\langle|\Delta v(l_s)|^2\rangle_N^{1/2} \sim 3.2 \pm 0.2$ mm/s, $\langle|\Delta v(l_s)|^2\rangle_L^{1/2} \sim 2.0 \pm 0.2$ mm/s. While H_z is close to the theoretical values $H_z = H_h/H_v = (1/3)/(3/5) \approx 0.56$, the sphero-scale is a bit smaller than the one estimated ($l_s \sim$ 4–80 cm) by *Lilley et al.* [2004], *Lovejoy et al.* [2009a], and *Lovejoy and Schertzer* [2010]. From H_z, we can estimate the vertical scaling exponent $\zeta_{v,N}(2) = \zeta_{h,N}(2)/H_{z,N} = 1.42 \pm 0.06$ and $\zeta_{v,L}(2) = \zeta_{h,L}(2)/H_{z,L} = 1.33 \pm 0.07$ values consistent with direct estimates of vertical exponents ($\zeta_v(2) \sim 1.35$ at 6 km) from drop sondes by *Lovejoy et al.* [2007]. Interestingly, while both the horizontal and vertical $\zeta(2)$ are little larger than the theoretical values (ignoring intermittency, 2/3, 6/5 respectively) yet, as expected, their ratio H_z is almost the same 0.8/1.4 = 0.57. These exponents are far from the theoretical values of 2D isotropic turbulence $\zeta_h(2) = 2$, $H_z = 0$. The overall fits (for $|\Delta z| < 40$ m and $|\Delta x| <$ 275 km) are shown in Figure 1, they are very good with mean relative deviations ±6% and ±4% (transverse, longitudinal respectively). Although the vertical range of scales is short, to our knowledge, Figure 1 constitutes the first direct estimate of the joint horizontal-vertical structure function; and it gives strong support to the hypothesis of horizontal-vertical anisotropic scaling.

5. Fractal Aircraft Trajectories

[13] In order to compare statistics at constant pressures and constant altitudes, we need to take into account the fractality of the aircraft trajectories. This fractality arises because aircraft at cruising altitudes fly on roughly isobaric levels and these are fractal [*Lovejoy et al.*, 2004], (although, due to inertia, at scales <3 km, the trajectories become smooth). This implies:

$$\langle|\Delta z(\Delta x)|\rangle \sim \left(\frac{\Delta x}{L_f}\right)^{H_{tr}} \langle|\Delta z(L_f)|\rangle \quad (5)$$

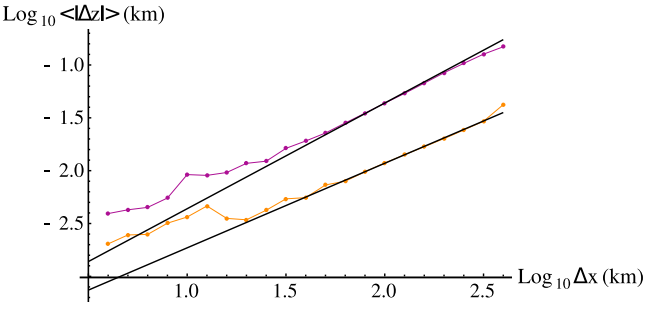

Figure 2. Mean vertical displacement as a function of horizontal separation. In orange: structure function calculated over near-constant pressure levels ($\Delta p < 1.26$ hPa). In purple: structure function calculated over near-constant pressure levels with an additional constraint on the slope ($\Delta z/\Delta x > 3 \times 10^{-4}$). Reference lines have slopes 0.8 and 1.0. The near-constant altitude (orange) curve shows a break in scaling symmetry for $\Delta x < 16$ km due to poor statistics.

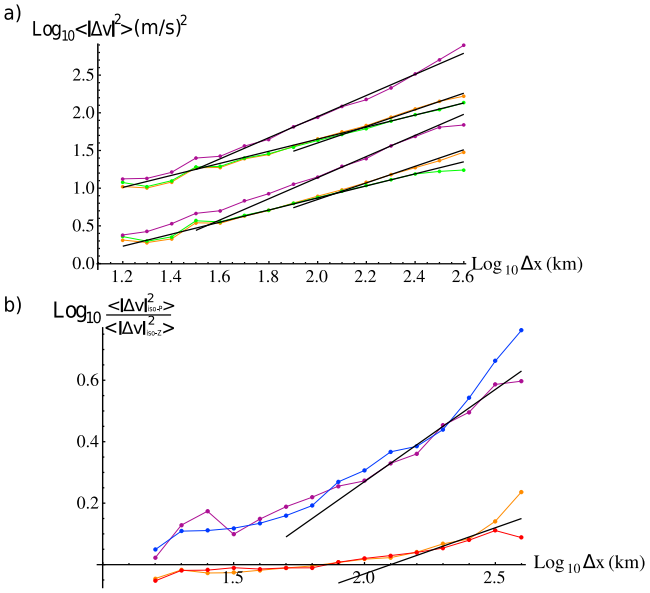

Figure 3. (a) $\langle|\Delta v(\Delta x, \Delta z)|^2\rangle$ for the transverse (upper curves) and longitudinal (lower curves) components of the wind measured by TAMDAR. The curves for transverse components were displaced in the vertical by 0.5 for clarity. In green: $\langle|\Delta v(\Delta x, \Delta z)|^2\rangle$ calculated over near-constant altitude levels ($\Delta z < 20$ m). In orange: $\langle|\Delta v(\Delta x, \Delta z)|^2\rangle$ calculated over near-constant pressure levels ($\Delta p < 1.26$ hPa). In purple: $\langle|\Delta v(\Delta x, \Delta z)|^2\rangle$ calculated over near-constant pressure levels with an additional constraint on the slope ($\Delta z/\Delta x > 3 \times 10^{-4}$). Reference lines have slopes 0.8, 1.1 and 1.4. (b) In orange (red): difference between logs of $\langle|\Delta v(\Delta x, \Delta z)|^2\rangle$ calculated on near-constant pressure and near-constant altitude levels for the transverse (longitudinal) component. In Purple (blue): difference between the logs of $\langle|\Delta v(\Delta x, \Delta z)|^2\rangle$ calculated on near-constant pressure with the additional constraint on the slope ($\Delta z/\Delta x > 3 \times 10^{-4}$) and near-constant altitude levels for the transverse (longitudinal) component. Reference lines have slopes 0.3 and 0.6.

where $\langle|\Delta z(\Delta x)|\rangle$ is the average vertical displacement of an aircraft over a horizontal lag Δx, $L_f \sim 180$ km is the average length of our TAMDAR flight segments, (chosen as a convenient reference scale) and $H_{tr} = D_{tr} - 1$ where D_{tr} is the fractal dimension of the "trajectory" (more precisely, it corresponds to the fractal dimension of the set of points on our isobaric sample). From Figure 2, we find $H_{tr} = 0.79 \pm 0.02$ and $\langle|\Delta z(L_f)|\rangle \sim 19 \pm 2$ m (which represents the average vertical displacement of the isobaric sample over L_f).

[14] To investigate the consequences for the velocity fluctuation statistics, we can use equation (2) and make a rough "mean field" type argument [see *Lovejoy et al.*, 2009a], where, in the scale function (equation (2)), we replace Δz with $\langle|\Delta z(\Delta x)|\rangle$ from equation (5):

$$\langle|\Delta v(\Delta x)|^2\rangle \sim \left\{\left|\frac{\Delta x}{l_s}\right| + \left|\frac{\Delta x}{\Delta x_0}\right|^{H_{tr}/H_z}\right\}^{\zeta_h(2)};$$

$$\Delta x_0 = L_f \left(\frac{l_s}{\langle|\Delta z(L_f)|\rangle}\right)^{1/H_{tr}} \quad (6)$$

Since $H_{tr} > H_z$, for isobars, there is a critical scale Δx_c for which, (taking $\zeta_v(2) = \zeta_h(2)/H_z \sim 0.8/0.57 \sim 1.4$):

$$\langle|\Delta v(\Delta x)|^2\rangle \sim |\Delta x|^{\zeta_h(2)} = |\Delta x|^{0.8} \; \Delta x \ll \Delta x_c;$$

$$\Delta x_c \sim (\Delta x_0^{H_{tr}} l_s^{-H_z})^{1/(H_{tr}-H_z)}$$

$$\langle|\Delta v(\Delta x)|^2\rangle \sim |\Delta x|^{H_{tr}\zeta_h(2)} = |\Delta x|^{1.1} \; \Delta x \gg \Delta x_c \quad (7)$$

The value of Δx_c depends on the turbulent fluxes (through the parameter l_s) and on Δx_0. Figure 3a compares the horizontal structure functions for near-constant pressure and altitude levels. As expected, the two curves are nearly identical for scales smaller than $\Delta x_{c,N} \sim 160$ km, $\Delta x_{c,L} \sim 125$ km, and follow a straight line with slope $\zeta_h(2) \sim 0.8$. As predicted, for scales larger than Δx_c, the near-isobaric (orange) curve follows a new line with slope $H_{tr}\zeta_v(2) \sim 1.1$. At the extreme large scale limit of our data (~300 km), there is a small deviation in the scaling of the longitudinal component. We checked that at this scale, there was a 25% difference in the contribution to $\langle|\Delta v_L(\Delta x)|^2\rangle$ for positive and negative Δv_L; since the aircraft mostly made round trips, this must be a consequence of the pilot modifying the trajectories depending on the weather – particularly affecting longitudinal components – hence introducing correlations between the aircraft and wind. By taking the ratio of the isobaric and isoaltitude $\langle|\Delta v|^2\rangle$ we largely eliminate this effect (Figure 3b): as predicted, the isoheight to isobar ratio continues to grow with scale with exponent ≈0.3.

[15] This $2 + H_z = 2.57$ dimensional turbulence has transverse to longitudinal ratio $D_{NN}/D_{LL} \sim 1.78 \pm 0.08$, somewhat higher than the theoretical 3D, 2D isotropic turbulence values ($D_{NN}/D_{LL} \sim 4/3$, 5/3, respectively [*Monin and Yaglom*, 1975; *Ogura*, 1952; *Lindborg*, 1999]).

[16] In order to further test the 23/9D theory, we show the results for data pairs constrained to have slopes $>3 \times 10^{-4}$ (roughly the mean isobaric slope at 400 km resolution), this sampling is linear ($H_{tr} \sim 1$, Figure 2) so that we expect exponents $H_{tr}\zeta_v(2) \sim 1.4$. This is confirmed by Figure 3a at scales >40 km. For these conditional isobaric curves, Figure 3a indicates $\Delta x_c \sim 36$ km, a value close to $\Delta x_c \sim 40$ km estimated using equation (7) and parameters estimated on Figures 1 and 2. Figure 3b shows the difference between isobaric (with and without the condition on the slopes of the sample) and near-constant altitude cases. For increasing horizontal lags, the difference between the isobaric and near-constant altitudes curves increase, showing the relevance of the 23/9D model and the effect of fractal trajectories/sampling as described by (equation (5)). Interestingly, the previous studies cited (from flights near the top of the troposphere, including Figures 1 and 2 of FS) find $\zeta(2) \sim 1.4$ so that presumably for these, $H_{tr} \sim 1$.

6. Conclusions

[17] The horizontal wind field is anomalous in that it has a break in the scaling at scales typically in the range 100–500 km with small scale spectra roughly $k^{-5/3}$ transitioning at lower wavenumbers to $\approx k^{-2.4}$. Both the transition scale and exponent are quite different from those predicted by theories of isotropic 3D and isotropic 2D turbulence (≈10 km and k^{-3}). A simple explanation is that the aircraft trajectories are gently sloping (e.g., they are isobaric) so that at a critical scale, the vertical fluctuations are dominant implying $k^{-2.4}$

for the sloping spectra (as in the vertical). In order to test this directly, high accuracy altitude and wind measurements are required; when carefully used the TAMDAR commercial aircraft sensors are adequate. However, due to degraded vertical resolution on ascending and descending flight segments, only cruise altitude data should be used and stringent pressure and altitude bounds are needed to define the isoheights and isobars ($\pm$10 m, $\pm$0.63 hPa).

[18] Using data from over 14500 flights, for the first time we were able to estimate the joint horizontal-vertical structure functions providing strong support to the 23/9 D anisotropic scaling theory (Figure 1), and estimating the key stratification exponent as $H_z = 0.57 \pm 0.02$, quite close to the theoretical value 5/9. Using this, and the observed fractal dimension of the isobars ($D_{tr} = 1.79 \pm 0.02$), we were able to theoretically calculate the isoheight, isobaric and constant slope structure function exponents (0.8, 1.1, 1.4 respectively) as well as the critical isoheight/isobar transition distance (≈160 km, 125 km, transverse, longitudinal). The results of this study give the strongest and most direct support to date for the 23/9D anisotropic scaling model.

[19] **Acknowledgments.** The Editor thanks the anonymous reviewer for helpful comments.

References

Charney, J. G. (1971), Geostrophic turbulence, *J. Atmos. Sci.*, *28*, 1087–1095, doi:10.1175/1520-0469(1971)028<1087:GT>2.0.CO;2.

Daniels, T. S., G. Tsoucalas, M. Anderson, D. Mulally, W. Moninger, and R. Mamrosh (2004), Tropospheric Airborne Meteorological Data Reporting (TAMDAR) sensor development, final report, NASA Langley Res. Cent., Hampton, Va.

Frehlich, R. G., and R. D. Sharman (2010), Equivalence of velocity statistics at constant pressure or constant altitude, *Geophys. Res. Lett.*, *37*, L08801, doi:10.1029/2010GL042912.

Kraichnan, R. H. (1967), Inertial ranges in two-dimensional turbulence, *Phys. Fluids*, *10*, 1417–1423, doi:10.1063/1.1762301.

Lilley, M., S. Lovejoy, K. Strawbridge, and D. Schertzer (2004), 23/9 dimensional anisotropic scaling of passive admixtures using lidar aerosol data, *Phys. Rev. E*, *70*, 036307, doi:10.1103/PhysRevE.70.036307.

Lindborg, E. (1999), Can the atmospheric kinetic energy spectrum be explained by two-dimensional turbulence?, *J. Fluid Mech.*, *388*, 259–288, doi:10.1017/S0022112099004851.

Lindborg, E., et al. (2009), Comment on "Reinterpreting aircraft measurements in anisotropic scaling turbulence" by Lovejoy et al. (2009), *Atmos. Chem. Phys. Discuss.*, *9*, 22,331–22,336, doi:10.5194/acpd-9-22331-2009.

Lindborg, E., et al. (2010), Interactive comment on "Comment on "Reinterpreting aircraft measurements in anisotropic scaling turbulence" by S. Lovejoy et al. (2009)," *Atmos. Chem. Phys. Discuss.*, *9*, 22,331–22,336.

Lovejoy, S., and D. Schertzer (2010), Towards a new synthesis for atmospheric dynamics: Space-time cascades, *Atmos. Res.*, *96*, 1–52, doi:10.1016/j.atmosres.2010.01.004.

Lovejoy, S., and D. Schertzer (2011), Space-time cascades and the scaling of ECMWF reanalyses: Fluxes and fields, *J. Geophys. Res.*, *116*, D14117, doi:10.1029/2011JD015654.

Lovejoy, S., D. Schertzer, and A. F. Tuck (2004), Fractal aircraft trajectories and nonclassical turbulent exponents, *Phys. Rev. E*, *70*(3), 036306, doi:10.1103/PhysRevE.70.036306.

Lovejoy, S., A. F. Tuck, S. J. Hovde, and D. Schertzer (2007), Is isotropic turbulence relevant in the atmosphere?, *Geophys. Res. Lett.*, *34*, L15802, doi:10.1029/2007GL029359.

Lovejoy, S., A. F. Tuck, D. Schertzer, and S. J. Hovde (2009a), Reinterpreting aircraft measurements in anisotropic scaling turbulence, *Atmos. Chem. Phys.*, *9*, 5007–5025, doi:10.5194/acp-9-5007-2009.

Lovejoy, S., A. F. Tuck, and D. Schertzer (2009b), Interactive comment on "Reinterpreting aircraft measurements in anisotropic scaling turbulence" by S. Lovejoy et al. (2009), *Atmos. Chem. Phys. Discuss.*, *9*, S2592–S2599.

Lovejoy, S., A. F. Tuck, and D. Schertzer (2009c), Interactive comment on "Comment on 'Reinterpreting aircraft measurements in anisotropic scaling turbulence' by Lovejoy et al. (2009)' by E. Lindborg et al., *Atmos. Chem. Phys. Discuss.*, *9*, C7688–C7699.

Lovejoy, S., A. F. Tuck, and D. Schertzer (2010), The Horizontal cascade structure of atmospheric fields determined from aircraft data, *J. Geophys. Res.*, *115*, D13105, doi:10.1029/2009JD013353.

Monin, A. S., and A. M. Yaglom (1975), *Statistical Fluid Mechanics: Mechanics of Turbulence*, vol. II, MIT Press, Cambridge, Mass.

Moninger, W. R., S. G. Benjamin, B. D. Jamison, T. W. Schlatter, T. L. Smith, and E. J. Szoke (2008), New TAMDAR fleets and their impact on Rapid Update Cycle (RUC) forecasts, paper presented at 13th Conference on Aviation, Range and Aerospace Meteorology, Am. Meteorol. Soc., New Orleans, La., 20–24 Jan.

Ogura, Y. (1952), The structure of two-dimensionally isotropic turbulence, *J. Meteorol. Soc. Jpn.*, *30*, 59–64.

Schertzer, D., and S. Lovejoy (1985a), The dimension and intermittency of atmospheric dynamics, *Turbul. Shear Flows*, *4*, 7–33, doi:10.1007/978-3-642-69996-2_2.

Schertzer, D., and S. Lovejoy (1985b), Generalised scale invariance in turbulent phenomena, *PhysicoChem. Hydrodyn.*, *6*, 623–635.

Schertzer, D., and S. Lovejoy (1987), Physical modeling and analysis of rain and clouds by anisotropic scaling multiplicative processes, *J. Geophys. Res.*, *92*, 9693–9714, doi:10.1029/JD092iD08p09693.

Schertzer, D., I. Tchigirinskaya, S. Lovejoy, and A. Tuck (2011), Quasi-geostrophic turbulence and generalized scale invariance, a theoretical reply, *Atmos. Chem. Phys. Discuss.*, *11*, 3301–3320, doi:10.5194/acpd-11-3301-2011.

Schertzer, D., I. Tchigirinskaya, S. Lovejoy, and A. Tuck (2012), Quasi-geostrophic turbulence and generalized scale invariance, a theoretical reply, *Atmos. Chem. Phys.*, *12*, 327–336, doi:10.5194/acp-12-327-2012.

Tuck, A. F. (2008), *Atmospheric Turbulence: A Molecular Dynamics Perspective*, Oxford Univ. Press, Oxford, U. K.

Van der Hoven, I. (1957), Power spectrum of horizontal wind speed in the frequency range from 0007 to 900 cycles per hour, *J. Meteorol.*, *14*, 160–164, doi:10.1175/1520-0469(1957)014<0160:PSOHWS>2.0.CO;2.

Yano, J. (2009), Comment on "Reinterpreting aircraft measurments in anisotropic scaling turbulence" by Lovejoy et al. (2009), *Atmos. Chem. Phys. Discuss.*, *9*, S162–S166.